Galectin-3 Activates PPARγ and Supports White Adipose Tissue Formation and High-Fat Diet-Induced Obesity

Jung-Hwan Baek, Seok-Jun Kim, Hyeok Gu Kang, Hyun-Woo Lee, Jung-Hoon Kim, Kyung-A Hwang, Jaewhan Song, and Kyung-Hee Chun

Department of Biochemistry and Molecular Biology (J.-H.B., S.-J.K., H.G.K., H.-W.L., K.-H.C.), Yonsei University College of Medicine, Seodaemun-gu, Seoul 120–752, Republic of Korea; Department of Biochemistry (H.-W.L., J.-H.K., J.S.), College of Life Science and Biotechnology, and Brain Korea 21 PLUS Project for Medical Science (J.-H.B., S.-J.K., H.G.K., K.-H.C.), Yonsei University, Seoul 120–749, Republic of Korea; and Department of Agrofood Resources (K.-A.H.), National Academy of Agricultural Science, Rural Development Administration, Suwon 441–857, Republic of Korea

Galectin-3, a β-galactoside-binding lectin, is elevated in obesity and type 2 diabetes mellitus, and metformin treatment reduces these galectin-3 levels. However, the role of galectin-3 in adipogenesis remains controversial. We found that 17-month-old galectin-3-deficient (lgals3$^{-/-}$) mice had decreased body size and epididymal white adipose tissue (eWAT) without related inflammatory diseases when fed normal chow. Galectin-3 knockdown significantly reduced adipocyte differentiation in 3T3-L1 cells and also decreased the expression of peroxisome proliferator-activated receptor (PPAR)-γ, ccaat-enhancer-binding protein α, and ccaat-enhancer-binding protein β. Endogenous galectin-3 directly interacted with PPARγ, and galectin-3 ablation reduced the nuclear accumulation and transcriptional activation of PPARγ. After a 12-week high-fat diet (60% fat), lgals3$^{-/-}$ mice had lower body weight and eWAT mass than lgals3$^{+/+}$ mice. Moreover, the expression of PPARγ and other lipogenic genes was drastically decreased in the eWAT and liver of lgals3$^{-/-}$ mice. We suggest that galectin-3 directly activates PPARγ and leads to adipocyte differentiation in vitro and in vivo. Furthermore, galectin-3 might be a potential therapeutic target in metabolic syndromes as a PPARγ regulator. (***Endocrinology*** **156: 147–156, 2015)**

A major role of white adipose tissue (WAT) is the maintenance of energy homeostasis through energy storage (1). When excessive food energy is taken in, the remaining energy is stored as triglycerides in WAT, increasing WAT mass. Too much WAT contributes to obesity, which is a metabolic disease that is associated with type 2 diabetes mellitus, hypertension, arteriosclerosis, and hyperlipidemia (2, 3). Peroxisome proliferator-activated receptor (PPAR)-γ is a nuclear receptor that plays a key role in lipid metabolism. PPARγ is activated by ligands, binds to the PPARγ response element (PPRE), and increases expression of target genes (4). PPARγ is a major transcription factor for adipocyte differentiation, and many studies have reported that PPARγ expression and activity regulate adipocyte differentiation (5, 6).

Galectin-3, a member of the animal lectin family, is a protein that contains a carbohydrate-recognition binding domain that binds to β-galactosides (7). Galectin-3 is ubiquitously localized in the nucleus, cytoplasm, and extracellular membrane and is involved in cell adhesion, cell cycle, apoptosis, inflammation, cell proliferation, and differentiation (8, 9). Because most studies on galectin-3 fo-

ISSN Print 0013-7227 ISSN Online 1945-7170
Printed in U.S.A.

Received May 7, 2014. Accepted October 16, 2014.
First Published Online October 24, 2014

Abbreviations: Acaca, acetyl-CoA carboxylase 1; acyl, acyltransferase; ATGL, adipose triglyceride lipase; C/EBP, ccaat-enhancer-binding protein; DMI, dexamethasone, 3-isobutyl-1-methylxanthine, and insulin; eWAT, epididymal white adipose tissue; FABP4, fatty acid binding protein 4; FAS, fatty acid synthase; FBS, fetal bovine serum; HA, hemagglutinin; HEK293, human embryonic kidney 293; IFN, interferon; KO, knockout; lgals3$^{-/-}$, galectin-3-deficient; Me1, NADP-dependent malic enzyme; MEF, mouse embryonic fibroblast; ORO, Oil-Red-O; PPAR, peroxisome proliferator-activated receptor; PPRE, PPARγ response element; SAT, sc adipose tissue; shRNA, small hairpin RNA; TG, triglyceride; VAT, visceral adipose tissue; WAT, white adipose tissue.

cus on cancer and inflammatory diseases, the role of galectin-3 in obesity is poorly understood. Galectin-3 is upregulated in growing adipose tissue and stimulates preadipocyte proliferation (10). Serum galectin-3 is elevated in obesity and is negatively correlated with glycated hemoglobin in type 2 diabetes (11). In mice with high-fat diet-induced obesity, expression of galectin-3 is increased in visceral adipose tissue (VAT) and sc adipose tissue (SAT) (12). Therefore, galectin-3 might be positively associated with obesity. However, contradictory results exist; adiposity, systemic inflammation, and abnormal glucose metabolism were increased in galectin-3 knockout (lgals3$^{-/-}$) mice (13). Lgals3$^{-/-}$ mice fed a high-fat diet have increased body weight, VAT mass, blood glucose, and insulin levels (14). This study suggests that accelerated high-fat diet-induced obesity in galectin-3 knockout (KO) mice is associated with amplified systemic inflammation. Body weight was significantly correlated with proinflammatory macrophages in the adipose tissue of lgals3$^{-/-}$ mice. However, these studies did not focus the regulation of adipocyte differentiation and fat accumulation.

We have elucidated the molecular mechanism of galectin-3 in vitro and in vivo during preadipocyte differentiation and in mice with high-fat diet-induced obesity. We have demonstrated that galectin-3 depletion down-regulates PPARγ expression and transcriptional activity. Lgals3$^{-/-}$ mice with high-fat diet-induced obesity had decreased body weight and adiposity without amplified inflammation, suggesting that galectin-3 might promote obesity through regulation of PPARγ.

Materials and Methods

Mice and diets

Male and female C57BL/6 mice with either a galectin-3 wild-type allele (homozygous$^{+/+}$) or a galectin-3-knockout allele (homozygous$^{-/-}$) were kindly provided by Dr F. T. Liu (University of California, Davis) (15). Wild-type and galectin-3-deficient mice were bred as heterozygotes in house and maintained on a C57BL/6 genetic background. Six-week-old male wild-type (lgals3$^{+/+}$) and galectin-3-deficient (lgals3$^{-/-}$) mice were fed a high-fat diet containing 60% fat for 12 weeks in the same room (12 h light, 12 h dark cycle). This experiment was independently performed with female lgals3$^{+/+}$ and lgals3$^{-/-}$ C57BL/6 mice. All mice used for studies were age matched but were not littermates. Body weight and food intake were measured once a week. All tissues were frozen in liquid nitrogen and stored at −80°C before analysis.

Cell culture and adipocyte differentiation assay

Human embryonic kidney 293 (HEK293) cells purchased from the Korea Cell Line Bank were cultured as described previously (16). The Korea Cell Line Bank authenticates the phenotypes of these cell lines. Heterozygous (lgals3$^{+/-}$) female and male N6 mice were crossed to produce lgals3$^{+/+}$ and lgals3$^{-/-}$ mouse embryonic fibroblasts (MEFs), as described previously (17). 3T3-L1 cells were grown to confluence, and differentiation was induced after 2 days with high glucose DMEM containing 10% fetal bovine serum (FBS), insulin (5 μg/mL), isobutylmethylxanthine (520 μM), and dexamethasone (1 μM). The media were replaced every 2 days with high-glucose DMEM containing 10% FBS and insulin (10 μg/mL) until day 8. MEF differentiation was induced with high-glucose DMEM containing 10% FBS, insulin (10 μg/mL), isobutylmethylxanthine (520 μM), dexamethasone (1 μM), and rosiglitazone (1 μM). MEF media were replaced every 2 days with high-glucose DMEM containing 10% FBS, insulin (10 μg/ml), and rosiglitazone (1 μM) until day 14 (18). Lipid accumulation was detected using Oil-Red-O staining (O0625; Sigma-Aldrich).

Generation of galectin-3 stable knockdown 3T3-L1 cells

Galectin-3 small hairpin RNA (shRNA)-lentiviral vectors were purchased from Sigma-Aldrich. Galectin-3 shRNA-lentiviruses were prepared as described previously (19). Briefly, HEK293FT cells were cotransfected with lentiviral and packaging vectors using Lipofectamine 2000 (Invitrogen). After 48 hours, media containing lentiviruses were harvested and filtered through 0.45-μm syringe filters. Lentiviruses were transduced in 50% confluent preadipocyte 3T3-L1 cells. Lentivirus-infected 3T3-L1 cells were selected by puromycin (2 μg/mL).

Western blot analysis

Cell lysate extractions were prepared with radioimmunoprecipitation assay buffer (1% Triton X-100; 1% sodium deoxycholate; 0.1% sodium dodecyl sulfate; 150 mM NaCl; 50 mM Tris-HCl, pH 7.5; and 2 mM EDTA, pH 8.0) and protease inhibitor cocktail (Genedepot). Cell lysates were incubated at 4°C for 20 minutes and centrifuged at 4°C for 25 minutes at 13 200 rpm. The supernatant concentration was measured with a Quibit 2.0 fluorometer (Invitrogen). Protein was loaded in SDS-PAGE gels, transferred to polyvinyl difluoride membrane (GE Healthcare), and blocked in 5% skim milk. Membranes were incubated with primary antibodies [galectin-3, ccaat-enhancer-binding protein (C/EBP)-α, C/EBPβ, PPARγ, fatty acid binding protein 4 (FABP4), hemagglutinin (HA; Santa Cruz Biotechnology), and Flag (Sigma-Aldrich)] at 4°C overnight in a rotor. Membranes were washed with PBS and Tween 20 and incubated with horseradish peroxidase-conjugated secondary antibodies (Santa Cruz Biotechnology). The LAS-3000 detector (Fujifilm) was used for image detection according to the manufacturer's directions. The normalization control was anti-β-actin (Santa Cruz Biotechnology).

Immunoprecipitation

Cell lysate extractions were performed with immunoprecipitation buffer and protease inhibitor cocktail (Genedepot). After centrifugation (13 200 rpm at 4°C for 25 min), the supernatants were added to protein A/G agarose beads (Santa Cruz Biotechnology) and incubated at 4°C for 30 minutes in a rotor for preclearing. After centrifugation (13 200 rpm at 4°C for 2 min), anti-Flag beads (Sigma-Aldrich), anti-galectin-3, anti-PPARγ,

and normal IgG (negative control) were independently added to supernatants and were then incubated at 4°C for overnight in a rotor. Immunoprecipitates were washed twice in immunoprecipitation buffer, added to 2× sodium dodecyl sulfate sample buffer, and boiled at 95°C for 5 minutes. After centrifugation (13 200 rpm at 4°C for 2 min), supernatants were analyzed by Western blot, as described previously (20).

Luciferase reporter assay

PPRE-TK-Luc, small hairpin galectin-3, and β-galactoside were cotransfected in HEK293 cells using Lipofectamine 2000 (Invitrogen). After 48 hours, cells were harvested and luciferase activities were measured using the luciferase assay system (Promega) as described previously (21). Luciferase activities were normalized by a β-galactoside enzyme assay system (Promega).

Immunocytochemistry

Immunocytochemistry was performed as described previously (22). Briefly, cells in chamber slides were fixed with 4% formaldehyde at 4°C for 30 minutes, washed with 1× PBS, and permeabilized in 0.5% Triton X-100 for 10 minutes. Cells were incubated with primary antibodies (galectin-3 and PPARγ) at 4°C and then were incubated with fluorescein isothiocyanate antimouse and Cy5 antirabbit secondary antibodies (Invitrogen) as well as 4′,6′-diamino-2-phenylindole staining solution (Vector Laboratories). Images were analyzed by confocal microscopy (LSM 700, Carl Zeiss).

RNA isolation and real-time RT-PCR analysis

Total tissue RNA was prepared using RNA-lysis reagent (5PRIME) as described previously (23). cDNA (1 μg) was synthesized from RNA by quantitative RT-PCR master mix (TOYOBO). The following primers were used: galectin-3, forward, 5′-cagtgctcctggaggctatc-3′, reverse, 5′-attgaagcgggggttaaagt-3′; PPARγ, forward, 5′-agggcgatcttgacaggaaa-3′, reverse, 5′-cgaaactggcacccttgaaa-3′; C/EBPα, forward, 5′-gtgactttgactaccgggga-3′, reverse, 5′-ggggctcttgtttgatcacc-3′; FABP4, forward, 5′-catcagcgtaaatggggatt-3′, reverse, 5′-tcgactttccatcccacttc-3′; fatty acid synthase (FAS), forward, 5′-tgggttctagccagcagagt-3′, reverse, 5′-accaccagagaccgttatgc-3′; adipose triglyceride lipase (ATGL), forward, 5′-caacgccactcacatctacg-3′, reverse, 5′-atgcagaggacccaggaa-3′; IL-10, forward, 5′-atcgatttctcccctgtgaa-3′, reverse, 5′-ttcggagagaggtacaaacga-3′; interferon (IFN)-γ, forward, 5′-gagccagattatctctttctacc-3′, reverse, 5′-gttgttgacctcaaacttgg-3′; TNFα, forward, 5′-cgtcagccgatttgctatct-3′, reverse, 5′-cggactccgcaaagtctaag-3′; and β-actin, forward, 5′-ggctgtattcccctccatcg-3′, reverse, 5′-ccagttggtaacaatgccatgt-3′. Real-time RT-PCR was performed using SYBR Green master mix (TOYOBO) with an ABI instrument (Applied Biosystems Inc). The normalization control was β-actin. Results were expressed compared with the average expression in wild-type (lgals3$^{+/+}$) mice.

Microarray analysis

Total liver RNA was prepared in RNA-lysis reagent (5PRIME). The gene expression was analyzed in cell lines using high-density oligonucleotide microarrays containing 20 889 transcripts (HG-U133 Plus 2.0; Affymetrix). Target preparation and microarray processing procedures were performed as described in the Affymetrix GeneChip expression analysis manual (Affymetrix). GeneChip analysis was carried out using the Affymetrix GeneChip manual with Microarray Analysis Suite 5.0, Data Mining Tool 2.0, and Microarray Database software. Microarray data analysis was performed as described previously (24).

Morphology analysis of epididymal white adipose tissue (eWAT)

eWAT samples were fixed in 4% paraformaldehyde and embedded in paraffin. eWAT paraffin sections were stained with hematoxylin and eosin. Images were analyzed using ImageJ software (National Institutes of Health, Bethesda, Maryland).

Triglyceride assay of eWAT

eWAT samples were homogenized in chloroform/methanol [2:1 (vol/vol)] as described previously (25). Briefly, 50 mM NaCl was added to tissue lysates, which were then vortexed for 10 minutes and centrifuged at 4°C for 10 minutes. The supernatant and interface were completely removed from the organic phase. Triton X-100/chloroform [7.5:17.5 (vol/vol)] were added, and the organic solvent was completely evaporated. Triglyceride (TG) levels were measured using a TG assay reagent (Thermo Scientific).

Statistical analysis

We used unpaired *t* tests to analyze comparisons between 2 groups. Statistical analysis was performed using GraphPad Prism 5.01. Values of $P < .05$ were considered significant.

Results

Seventeen-month-old lgals3$^{-/-}$ mice have reduced WAT

Seventeen-month-old male lgals3$^{-/-}$ mice (n = 5) were significantly smaller than wild-type (lgals3$^{+/+}$) mice (Figure 1A). The eWAT was also drastically lessened in lgals3$^{-/-}$ mice (Figure 1B). Moreover, lgals3$^{-/-}$ mice exhibited a lower eWAT weight to body weight ratio than wild-type (lgals3$^{+/+}$) mice (Figure 1C). However, there was no significant difference in the size of brown adipose tissues or the liver between groups (Figure 1, D and E). Therefore, we measured the expression of genes related to adipogenesis or lipogenesis in the eWAT and in the liver. Interestingly, the mRNA expression of PPARγ and FABP4 was reduced in eWAT in lgals3$^{-/-}$ mice (Figure 1F). Even though the liver size was unchanged, the mRNA expression of PPARγ and FAS was reduced in the liver of lgals3$^{-/-}$ mice, indicating that galectin-3 deficiency down-regulates the expression of adipogenic and lipogenic genes in both eWAT and liver (Figure 1H). Interestingly, the expression levels of IL-10, IFNγ, and TNFα were unchanged in both eWAT and the liver of lgals3$^{-/-}$ mice, suggesting that the amplified inflammation did not occur in lgals3$^{-/-}$ mice (Figure 1, G and I).

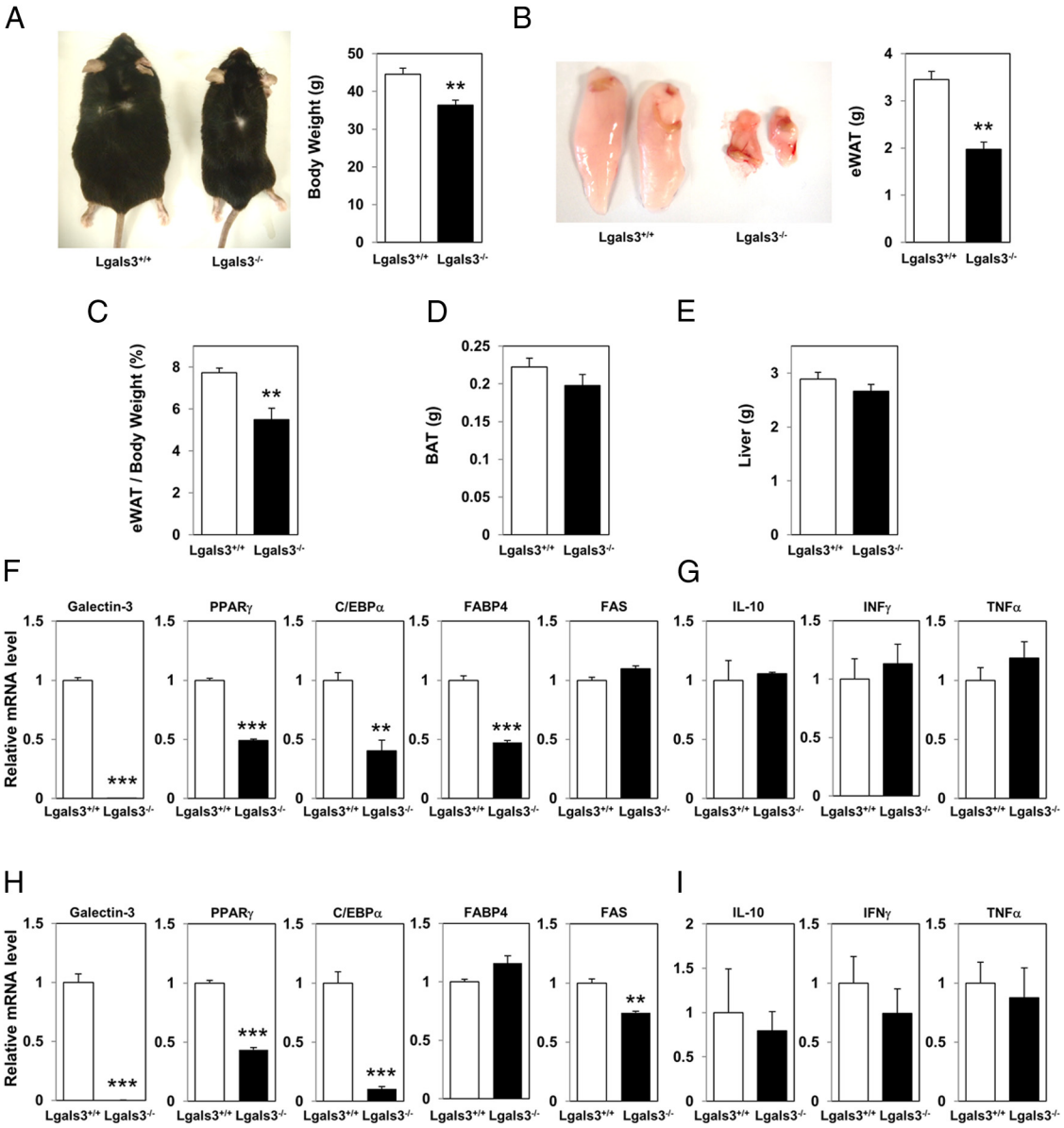

Figure 1. Seventeen-month-old lgals3$^{-/-}$ mice have reduced WAT. A, Decreased body size and weight of lgals3$^{-/-}$ mice fed chow. Representative picture of wild-type and lgals3$^{-/-}$ mice fed chow for 17 months. B, Size and weight of eWAT. C, eWAT weight per body weight. D, Weight of brown adipose tissue. E, Weight of liver. F, Real-time RT-PCR analysis of genes in eWAT. G, Real-time RT-PCR analysis of IL-10, IFNγ, and TNFα in eWAT. H, Real-time RT-PCR analysis of liver genes including galectin-3, PPARγ, C/EBPα, FABP4, and FAS. I, Real-time RT-PCR analysis of IL-10, IFNγ, and TNFα in the liver. mRNA expression was normalized to β-actin. Data are presented as mean ± SEM (n = 5 for wild-type and lgals3$^{-/-}$ mice fed chow). *, $P < .05$, **, $P < .01$, and ***, $P < .001$ for wild-type vs lgals3$^{-/-}$ mice. BAT, brown adipose tissue.

lgals3$^{-/-}$ MEFs exhibit retardation of adipocyte differentiation

Because the expression of adipogenic and lipogenic genes was reduced in lgals3$^{-/-}$ mice, we hypothesized that galectin-3 might play an important role in adipogenesis. The lgals3$^{+/+}$ and lgals3$^{-/-}$ MEFs were treated with dexamethasone, 3-isobutyl-1-methylxanthine, and insulin (DMI) and rosiglitazone, which induced adipocyte differentiation. The intensity of adipocyte differentiation was measured with Oil-Red-O (ORO) staining of lipid droplets. For up to 14 days, adipocyte differentiation in lgals3$^{-/-}$ MEFs was retarded compared with control lgals3$^{+/+}$ MEFs (Figure 2, A and B). Adipocyte-differentiated lgals3$^{-/-}$ MEFs had fewer total lipids than adipocyte-differentiated lgals3$^{+/+}$ MEFs (Figure 2C). The expression of PPARγ, C/EBPα, C/EBPβ, and FABP4 was reduced in adipocyte-differentiated lgals3$^{-/-}$ MEFs (Figure 2D).

Galectin-3-depleted 3T3-L1 cells exhibit retardation of adipocyte differentiation

We determined the effect of galectin-3 on the differentiation of preadipocyte 3T3-L1 cells. The levels of galec-

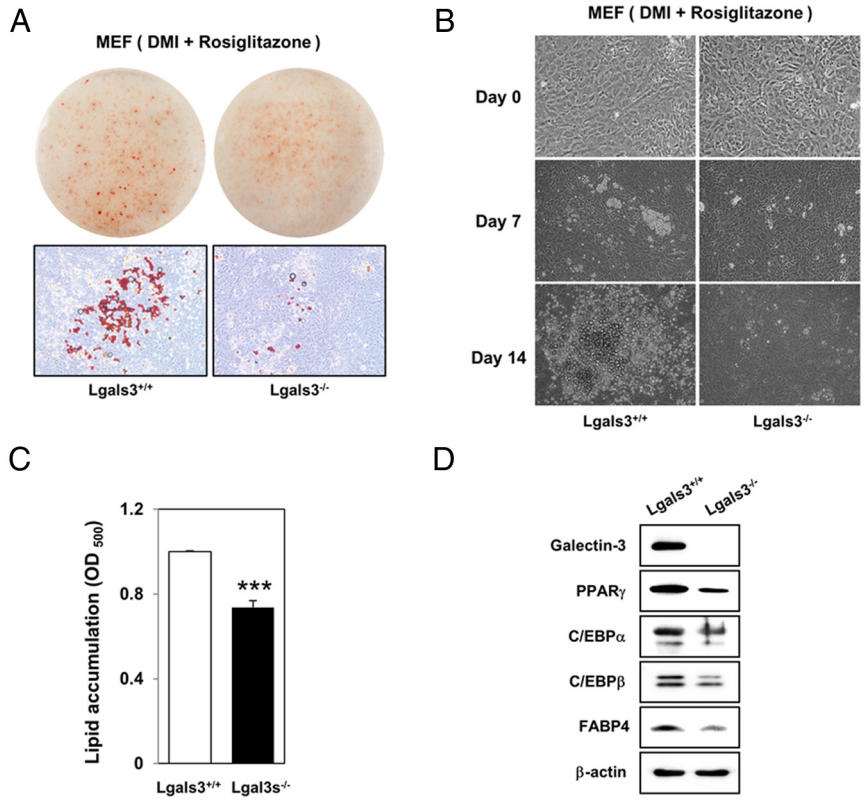

Figure 2. lgals3$^{-/-}$ MEFs exhibit retardation of adipocyte differentiation. A and B, Adipocyte differentiation of wild-type and lgals3$^{-/-}$ MEFs. MEFs were treated with DMI and rosiglitazone for 14 days. We performed ORO staining on adipocytes. C, Measurement of lipid accumulation. Stained ORO dye was eluted by 100% isopropanol and measured using the OD_{500}. D, Western blot analysis of adipogenic factors in wild-type and lgals3$^{-/-}$ MEFs. Protein expression of adipogenic factors was normalized to β-actin. Data are presented as mean ± SEM (n = 3 for each lane). ***, $P < .001$ for wild-type vs lgals3$^{-/-}$ MEFs.

tin-3 mRNA and protein increased during adipocyte differentiation (Figure 3, A and B). To identify the role of galectin-3 in adipocyte differentiation, we stably silenced galectin-3 expression in 3T3-L1 cells. The 3T3-L1 cells were infected with galectin-3 shRNA lentiviruses, and galectin-3 depletion was confirmed in shRNAs 2 and 5 (Figure 3C). The 3T3-L1 cells were induced with DMI and differentiated for 8 days. Galectin-3-depleted 3T3-L1 cells showed significantly delayed adipocyte differentiation and lipid accumulation, compared with control 3T3-L1 cells (Figure 3, D and E). Consequently, they had a low expression of PPARγ, C/EBPα, C/EBPβ, and FABP4 (Figure 3F). These data suggest that galectin-3 might be a positive regulator of adipocyte differentiation.

Galectin-3 interacts with PPARγ and increases its transcriptional activity

We investigated the interaction between galectin-3 and PPARγ. HEK293 cells were cotransfected with FLAG-tagged galectin-3 and HA-tagged PPARγ. After 48 hours, cells were harvested and cell lysates were immunoprecipitated using anti-FLAG beads. We confirmed interactions between exogenously expressed Flag-galectin-3 and HA-PPARγ in HEK293 cells by Western blot with anti-Flag and anti-HA antibodies (Figure 4A). Furthermore, interaction between endogenous galectin-3 and PPARγ was confirmed in 3T3-L1 cells (Figure 4B). To determine the effect of galectin-3 on PPARγ transcriptional activity, galectin-3 was knocked down by shRNA in HEK293 cells with a transiently transfected PPRE reporter in the absence or presence of rosiglitazone, a PPARγ agonist (Figure 4C). Galectin-3 depletion significantly reduced PPARγ transcriptional activity with and without rosiglitazone compared with small hairpin LacZ. Using immunocytochemistry, we found that the expression and nuclear localization of PPARγ were decreased by galectin-3 silencing in 3T3-L1 cells (Figure 4D). These data suggest that galectin-3 might positively regulate PPARγ expression and transcriptional activity by direct interaction.

lgals3$^{-/-}$ mice are resistant to high-fat diet-induced obesity

We fed a high-fat diet containing 60% fat to male lgals3$^{+/+}$ and lgals3$^{-/-}$ mice (n = 5) for 12 weeks and characterized the phenotypes. Male lgals3$^{-/-}$ mice had a lower body weight than lgals3$^{+/+}$ mice (Figure 5, A and B, Supplemental Figure 1), even though food intake did not differ between these 2 groups (Figure 5C). Moreover, lgals3$^{-/-}$ mice exhibited less eWAT and a lower eWAT weight to body weight ratio than lgals3$^{+/+}$ mice (Figure 5, D and E), suggesting that high-fat diet-induced obesity was induced less in lgals3$^{-/-}$ mice. However, brown adipose tissues and liver weight were not statistically different between these 2 groups (Figure 5, F and G). We independently experimented with high-fat diet-induced obesity in female lgals3$^{-/-}$ mice (Supplemental Figure 2). Although body weight was not statistically different between female lgals3$^{+/+}$ and lgals3$^{-/-}$ mice, we obtained similar results regarding body weight, eWAT weight, and the ratio of eWAT to body weight.

Many reports indicate that obesity is related to the risk of type 2 diabetes mellitus and hyperlipidemia (2, 3). We

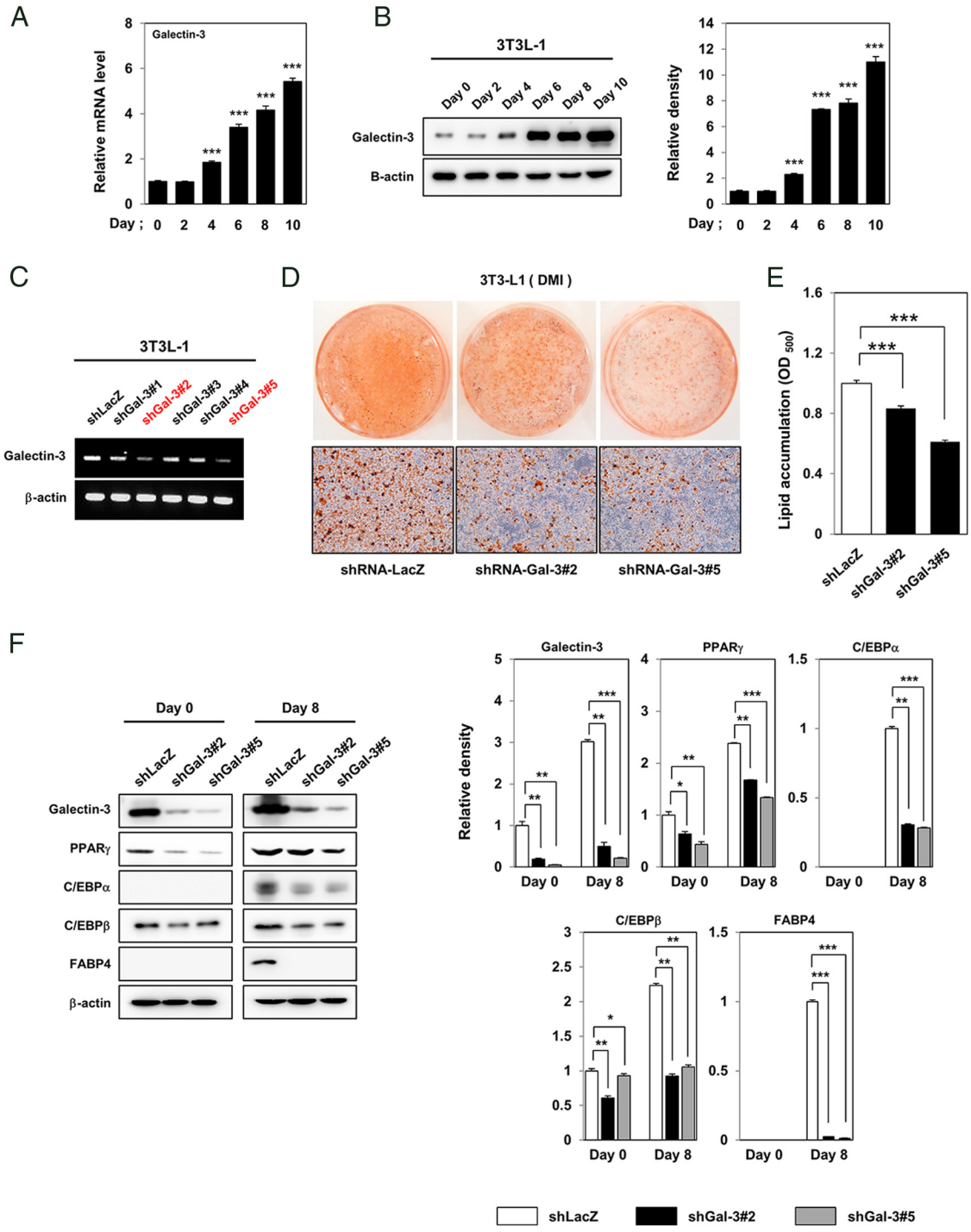

Figure 3. Galectin-3-depleted 3T3-L1 cells exhibit retardation of adipocyte differentiation. A, Level of galectin-3 mRNA during adipocyte differentiation. B, Level of galectin-3 protein during adipocyte differentiation. C, Galectin-3 stably silenced 3T3-L1 cells. The 3T3-L1 cells were infected with galectin-3 shRNA lentiviruses (pLKO.1-puro vector) and selected by puromycin. D, Adipocyte differentiation of galectin-3 stably silenced 3T3-L1 cells. Cells were treated with DMI for 8 days, and we performed ORO staining on adipocytes. E, Measurement of lipid accumulation. Stained ORO dye was eluted with 100% isopropanol and measured using the OD_{500}. F, Western blot analysis of adipogenic factors in galectin-3 stably silenced 3T3-L1 cells and relative density as quantified by ImageJ software (National Institutes of Health). Protein expression of adipogenic factors was normalized to β-actin. Data are presented as mean ± SEM (n = 3 for each lane). *, $P < .05$, **, $P < .01$, and ***, $P < .001$ for small hairpin LacZ vs small hairpin galectin-3, -2, and -5. sh, small hairpin.

examined the regulation of blood glucose and plasma free fatty acids in lgals3$^{-/-}$ mice (Figure 5, H and I). Despite increased body weight and adiposity in lgals3$^{+/+}$ mice, fasting blood glucose and plasma free fatty acids were not statistically different between lgals3$^{+/+}$ and lgals3$^{-/-}$ mice.

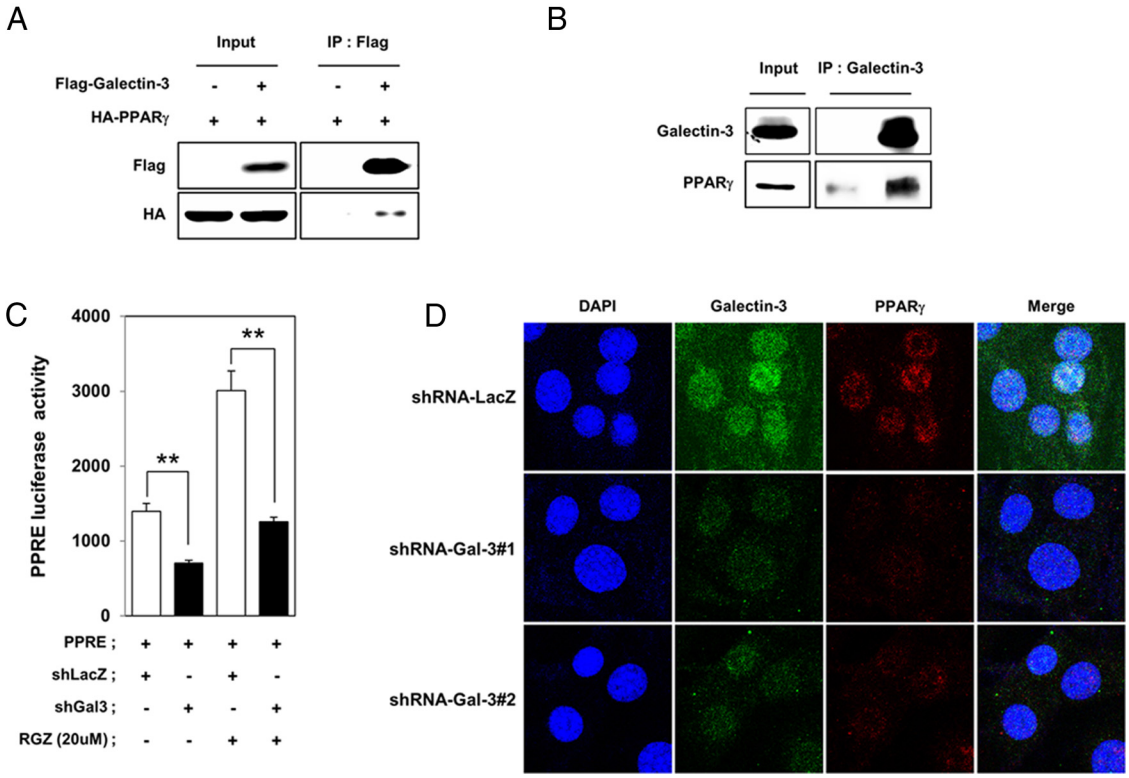

Figure 4. Galectin-3 interacts with PPARγ and increases its transcriptional activity. A, Coimmunoprecipitation of exogenous galectin-3 (Flag tagged) and PPARγ (HA tagged) in HEK293 cells. Cell lysates were immunoprecipitated using anti-Flag beads. B, Coimmunoprecipitation of endogenous galectin-3 and PPARγ in 3T3-L1 cells. C, Luciferase activities of PPRE in HEK293 cells. HEK293 cells were cotransfected with small hairpin galectin-3, PPRE, and β-galactoside and then treated with 20 μM rosiglitazone. Luciferase activities were normalized to β-galactoside activity. D, Immunocytochemistry of galectin-3 and PPARγ in galectin-3 stably silenced 3T3-L1 cells. Data are presented as mean ± SEM (n = 3 for each lane). *, $P < .05$ and **, $P < .01$ for small hairpin LacZ vs small hairpin galectin-3. DAPI, 4′,6′-diamino-2-phenylindole; sh, small hairpin.

lgals3$^{-/-}$ mice exhibit decreased adiposity and altered ATGL expression in eWAT

We detected a reduced adipocyte size in eWAT of lgals3$^{-/-}$ mice fed a high-fat diet (Figure 6A), indicating that reduced adiposity in eWAT was not due to a decrease in adipocyte number. High-fat diet-induced TG levels were also lower in the eWAT of lgals3$^{-/-}$ mice (Figure 6B). Interestingly, the expression of ATGL was significantly increased in the eWAT of lgals3$^{-/-}$ mice fed a high-fat diet (Figure 6C). Taken together, we found that a reduced adipocyte size in the eWAT of lgals3$^{-/-}$ mice fed a high-fat diet was caused by increased ATGL levels. Further study is required to confirm the regulation of ATGL by galectin-3.

lgals3$^{-/-}$ mice have altered hepatic lipogenic gene expression

Fatty liver diseases are often exhibited in obesity, but a histological analysis of the livers showed no difference between the lgals3$^{+/+}$ and lgals3$^{-/-}$ mice in this study. Therefore, we measured expression of lipogenic genes in liver tissues by a DNA microarray analysis. The mRNA expression of PPARγ, C/EBPα, FABP4, FAS, NADP-dependent malic enzyme (Me1), acetyl-CoA carboxylase 1 (Acaca), acyltransferase (Acyl), and Slc25a1 was reduced in the liver tissues of lgals3$^{-/-}$ mice (Figure 6D). We also used a real-time RT-PCR analysis to confirm that mRNA expression of PPARγ, C/EBPα, FABP4, and FAS was relatively low in liver tissues of lgals3$^{-/-}$ mice (Figure 6E). This suggests that galectin-3 might influence lipogenic genes in the liver, stimulating systemic obesity.

Discussion

We suggest that galectin-3 might be a positive regulator of high-fat diet-induced obesity. This is in agreement with previous reports demonstrating that galectin-3 is up-regulated during adipocyte differentiation and in obesity (10). Serum galectin-3 was elevated in obese patients and was negatively correlated with glycated hemoglobin in type 2 diabetes (11). In mice with high-fat diet-induced obesity, galectin-3 levels increased in VAT and SAT (12). However, other groups reported that galectin-3 KO mice have increased adiposity. Young galectin-3 KO mice de-

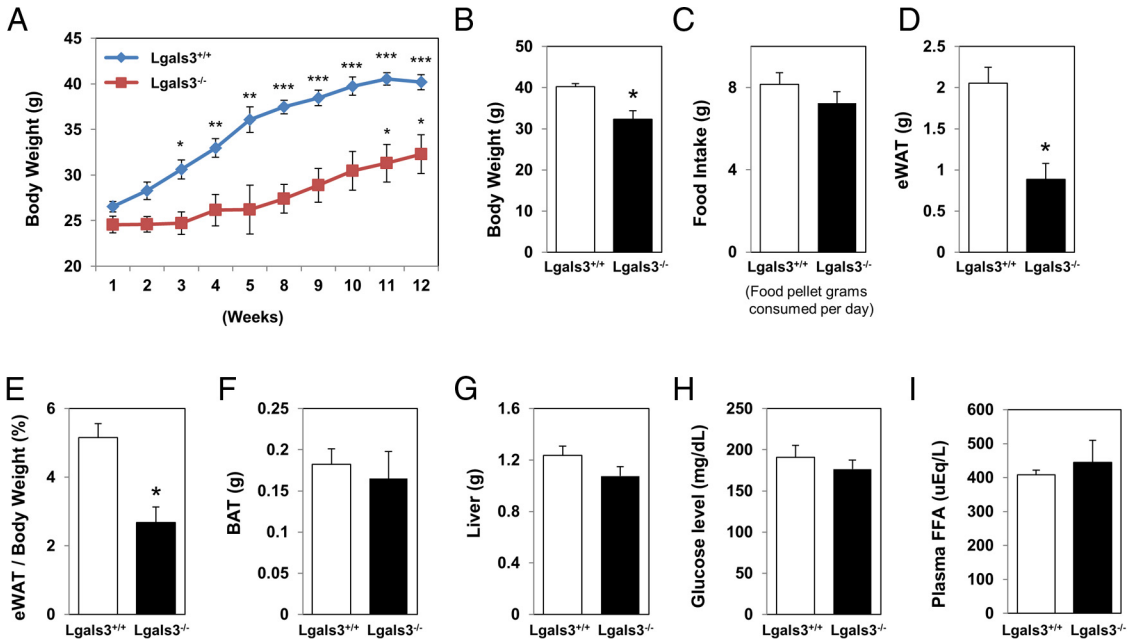

Figure 5. lgals3$^{-/-}$ mice are resistant to high-fat diet-induced obesity. A and B, Body weight of wild-type and lgals3$^{-/-}$ mice fed a high-fat diet (60% fat) for 12 weeks. C, Grams of food pellets consumed per day. D, Weight of eWAT. E, eWAT weight per body weight. F, Weight of brown adipose tissue. G, Weight of liver. H, Blood glucose levels, measured after 5 hours of fasting. I, Level of plasma free fatty acids. Data are presented as mean ± SEM (n = 5 for wild-type and lgals3$^{-/-}$ mice fed a high fat diet). *, $P < .05$ for wild-type vs lgals3$^{-/-}$ mice. BAT, brown adipose tissue.

veloped mild hyperglycemia followed by increased adiposity and systemic inflammation (13). Fasting blood glucose levels were normalized by antibiotic treatment in lgals3$^{-/-}$ mice. This study pointed to a potential role of microbiota as the cause of hyperglycemia in lgals3$^{-/-}$ mice. Galectin-3 deficiency induced systemic inflammation, increasing proinflammatory macrophages, type 1 T cells, and NKT cells while decreasing regulatory T cells and M2 macrophages (14). Body weight was correlated with proinflammatory macrophages and inversely correlated with regulatory T cells in the adipose tissue of lgals3$^{-/-}$ mice. They described that increased high-fat diet-induced obesity of lgals3$^{-/-}$ mice is associated with systemic inflammation. The change in the balance between T_H1 and T_H2 cells in adipose tissues affects recruitment of activated macrophages, inflammatory response, and regulation of body weight (26). However, these studies did not focus on whether galectin-3 deficiency regulates the expression and activity of genes regulating adipocyte differentiation and fat accumulation. We examined the regulation of adipogenic factors by galectin-3. We did not observe symptoms of amplified inflammation in our galectin-3-deficient mice, possibly due to their different living environment.

Seventeen-month-old lgals3$^{-/-}$ mice are lean compared with wild-type (lgals3$^{+/+}$) mice fed with normal chow. These lgals3$^{-/-}$ mice had decreased eWAT size as well as decreased expression of adipogenic and lipogenic genes in the eWAT and liver. We therefore explored whether galectin-3 regulates the expression and/or activity of PPARγ, a known master regulator of adipocyte differentiation and lipid metabolism (4, 16). Galectin-3-depleted preadipocyte 3T3-L1 cells exhibited delayed adipocyte differentiation and decreased expression of adipogenic genes, such as PPARγ, C/EBPα, and C/EBPβ. Moreover, the adipocyte differentiation of lgals3$^{-/-}$ MEFs was delayed compared with the wild-type (lgals3$^{+/+}$) cells. Interestingly, galectin-3 directly interacted with PPARγ and regulated its expression and transcriptional activation. This suggests that galectin-3 plays a direct role in adipogenesis through PPARγ regulation.

Furthermore, we demonstrated that galectin-3 might be a positive regulator of high-fat diet-induced obesity. This is in agreement with reports demonstrating that galectin-3 is up-regulated during adipocyte differentiation and in obesity (10). We fed 6-week-old lgals3$^{+/+}$ and lgals3$^{-/-}$ mice high-fat chow (60% fat) for 12 weeks. The lgals3$^{-/-}$ mice had reduced body weight and eWAT mass compared with wild-type (lgals3$^{+/+}$) mice, suggesting that galectin-3 deficiency increases resistance to high-fat diet-induced obesity. Interestingly, fat accumulation in the liver as measured by histological analysis and TG content did not differ between lgals3$^{+/+}$ and lgals3$^{-/-}$ mice. A DNA microarray analysis revealed that adipogenic and lipogenic genes, such as PPARγ, C/EBPα, FABP4, FAS, Me1, Acaca, Acyl, and Slc25a1 were reduced in liver tissues of lgals3$^{-/-}$ mice. These genes uptake free fatty acids and synthesize lipids in the liver (27). Up-regulation of

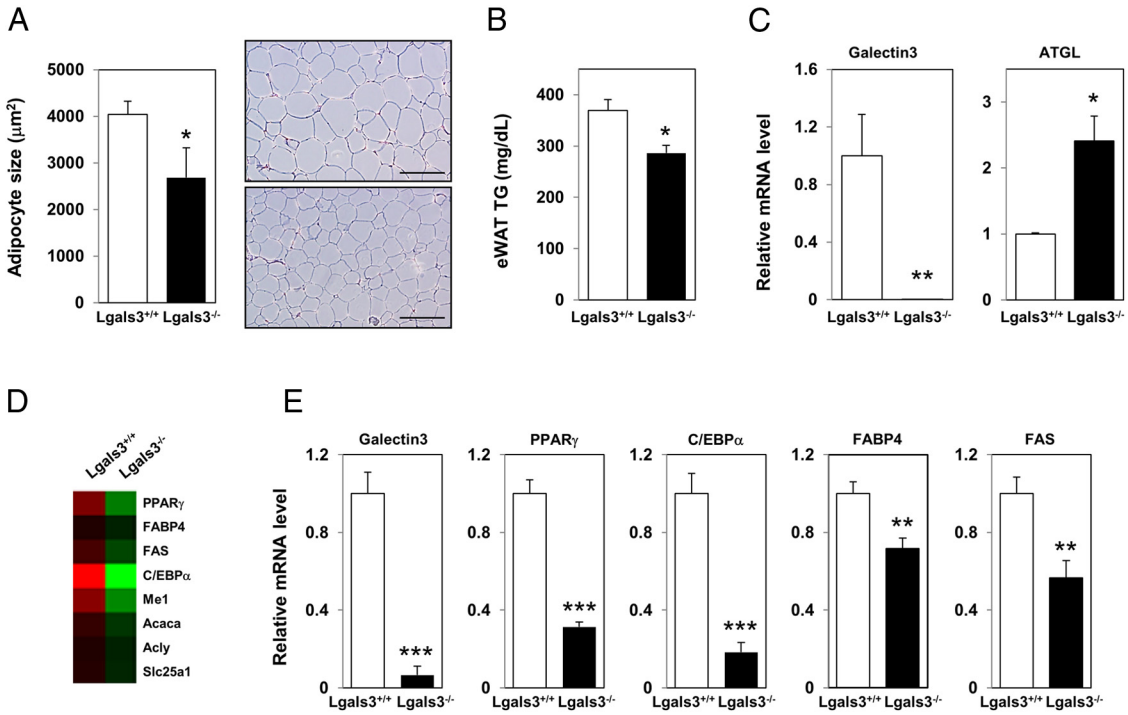

Figure 6. lgals3$^{-/-}$ mice exhibit decreased adiposity and altered ATGL expression in eWAT. A, Adipocyte size of eWAT sections stained with hematoxylin and eosin (H&E). Size measurement was performed using ImageJ software (National Institutes of Health). B, TG content in eWAT. TG accumulation was measured with a TG assay kit. C, Real-time RT-PCR analysis of galectin-3 and ATGL in eWAT. D, Microarray analysis of liver tissue showed decreased expression of PPARγ, C/EBPα, FABP4, FAS, Me1, Acaca, Acyl, and Slc25a1. E, Real-time RT-PCR analysis of genes in the liver, including galectin-3, PPARγ, C/EBPα, FABP4, and FAS. mRNA expression of lipogenic factors was normalized to β-actin. Data are presented as mean ± SEM (n = 5 for wild type and lgals3$^{-/-}$ mice fed a high fat diet). *, $P < .05$, **, $P < .01$, and ***, $P < .001$ for wild-type vs lgals3$^{-/-}$ mice.

lipogenic genes contributes to excessive TG accumulation in the liver as well as fatty liver diseases. Previous reports demonstrated that galectin-3 deficiency inhibited hepatic fibrosis (28, 29) and protected against nonalcoholic steatohepatitis (30, 31), suggesting that galectin-3 might be a therapeutic target in liver diseases, such as fatty liver, steatosis, and cirrhosis, through the regulation of lipid accumulation and fibrosis. However, the disruption of galectin-3 can cause nonalcoholic fatty liver disease (32). Although we could not detect any serious liver abnormalities in lgals3$^{+/+}$ mice, the change observed in lipogenic genes is sufficient evidence indicating that overexpression of galectin-3 in liver may induce liver disease.

In lgals3$^{-/-}$ mice fed a high-fat diet, adipocyte size and lipid accumulation were decreased in the eWAT of galectin-3 KO mice. PPARγ and lipogenic genes were also down-regulated in the eWAT of lgals3$^{-/-}$ mice. Interestingly, ATGL was significantly increased in the eWAT of lgals3$^{-/-}$ mice. ATGL is an enzyme that catalyzes the rate-limiting hydrolysis step of TGs in the triacylglycerol lipolysis cascade (33). In the absence of ATGL, mice increase WAT mass and TG deposition in multiple tissues. The ATGL KO mice had increased adiposity and TG storage in WAT (34). This suggests that decreased adiposity in the lgals3$^{-/-}$ mice might be due to an increased expression of ATGL. Future research will investigate the mechanism by which galectin-3 regulates ATGL expression.

Taken together, our data suggest that galectin-3 plays an important role in adipogenesis and high-fat diet-induced obesity. Therefore, targeting galectin-3 might improve therapies for metabolic diseases.

Acknowledgments

Address all correspondence and requests for reprints to: Kyung-Hee Chun PhD, Department of Biochemistry and Molecular Biology, Yonsei University College of Medicine, 50 Yonsei-ro, Seodaemun-gu, Seoul 120–752, Republic of Korea. E-mail: khchun@yuhs.ac.

This work was supported by the Cooperative Research Program for Agricultural Science and Technology Development (Grant PJ008462) and by the National Research Foundation of Korea Grant NRF-2011–0030086 funded by the Korea Government.

Disclosure Summary: The authors have nothing to disclose.

References

1. **Spiegelman BM, Flier JS.** Obesity and the regulation of energy balance. *Cell*. 2001;104(4):531–543.
2. **Steinberger J, Daniels SR, American Heart Association Atherosclerosis, Hypertension, and Obesity in the Young Committee (Council on Cardiovascular Disease in the Young); American Heart Association Diabetes Committee (Council on Nutrition, Physical Activity, and Metabolism).** Obesity, insulin resistance, diabetes, and cardiovascular risk in children: an American Heart Association scientific statement from the Atherosclerosis, Hypertension, and Obesity in the Young Committee (Council on Cardiovascular Disease in the Young) and the Diabetes Committee (Council on Nutrition, Physical Activity, and Metabolism). *Circulation*. 2003;107(10):1448–1453.
3. **Carr MC, Brunzell JD.** Abdominal obesity and dyslipidemia in the metabolic syndrome: importance of type 2 diabetes and familial combined hyperlipidemia in coronary artery disease risk. *J Clin Endocrinol Metab*. 2004;89(6):2601–2607.
4. **Ahmadian M, Suh JM, Hah N, et al.** PPARγ signaling and metabolism: the good, the bad and the future. *Nat Med*. 2013;19(5):557–566.
5. **Kim TH, Kim MY, Jo SH, Park JM, Ahn YH.** Modulation of the transcriptional activity of peroxisome proliferator-activated receptor γ by protein-protein interactions and post-translational modifications. *Yonsei Med J*. 2013;54(3):545–559.
6. **Dutchak PA, Katafuchi T, Bookout AL, et al.** Fibroblast growth factor-21 regulates PPARγ activity and the antidiabetic actions of thiazolidinediones. *Cell*. 2012;148(3):556–567.
7. **Dumic J, Dabelic S, Flogel M.** Galectin-3: an open-ended story. *Biochim Biophys Acta*. 2006;1760(4):616–635.
8. **Liu FT, Rabinovich GA.** Galectins as modulators of tumour progression. *Nat Rev Cancer*. 2005;5(1):29–41.
9. **Henderson NC, Sethi T.** The regulation of inflammation by galectin-3. *Immunol Rev*. 2009;230(1):160–171.
10. **Kiwaki K, Novak CM, Hsu DK, Liu FT, Levine JA.** Galectin-3 stimulates preadipocyte proliferation and is up-regulated in growing adipose tissue. *Obesity*. 2007;15(1):32–39.
11. **Weigert J, Neumeier M, Wanninger J, et al.** Serum galectin-3 is elevated in obesity and negatively correlates with glycosylated hemoglobin in type 2 diabetes. *J Clin Endocrinol Metab*. 2010;95(3):1404–1411.
12. **Rhodes DH, Pini M, Castellanos KJ, et al.** Adipose tissue-specific modulation of galectin expression in lean and obese mice: evidence for regulatory function. *Obesity*. 2013;21(2):310–319.
13. **Pang J, Rhodes DH, Pini M, et al.** Increased adiposity, dysregulated glucose metabolism and systemic inflammation in Galectin-3 KO mice. *PloS One*. 2013;8(2):e57915.
14. **Pejnovic NN, Pantic JM, Jovanovic IP, et al.** Galectin-3 deficiency accelerates high-fat diet-induced obesity and amplifies inflammation in adipose tissue and pancreatic islets. *Diabetes*. 2013;62(6):1932–1944.
15. **Hsu DK, Yang RY, Pan Z, et al.** Targeted disruption of the galectin-3 gene results in attenuated peritoneal inflammatory responses. *Am J Pathol*. 2000;156(3):1073–1083.
16. **Kim SJ, Hwang JA, Ro JY, Lee YS, Chun KH.** Galectin-7 is epigenetically-regulated tumor suppressor in gastric cancer. *Oncotarget*. 2013;4(9):1461–1471.
17. **Ko A, Shin JY, Seo J, et al.** Acceleration of gastric tumorigenesis through MKRN1-mediated posttranslational regulation of p14ARF. *J Natl Cancer Inst*. 2012;104(21):1660–1672.
18. **Kim JH, Park KW, Lee EW, et al.** Suppression of PPARγ through MKRN1-mediated ubiquitination and degradation prevents adipocyte differentiation. *Cell Death Differ*. 2014;21(4):594–603.
19. **Kim SJ, OH JS, Shin JY, et al.** Development of microRNA-145 for therapeutic application in breast cancer. *J Control Release*. 2011;155(3):427–434.
20. **Kim SJ, Shin JY, Cheong TC, Cet al.** Galectin-3 germline variant at position 191 enhances nuclear accumulation and activation of beta-catenin in gastric cancer. *Clin Exp Metastasis*. 2011;28(8):743–750.
21. **Wang YG, Kim SJ, Baek JH, Lee HW, Jeong SY, Chun KH.** Galectin-3 increases the motility of mouse melanoma cells by regulating matrix metalloproteinase-1 expression. *Exp Mol Med*. 2012;44(6):387–393.
22. **Kim SJ, Choi IJ, Cheong TC, et al.** Galectin-3 increases gastric cancer cell motility by up-regulating fascin-1 expression. *Gastroenterology*. 2010;138(3):1035–1045.
23. **Ahn YH, Yi H, Shin JY, et al.** STAT3 silencing enhances the efficacy of the HSV.tk suicide gene in gastrointestinal cancer therapy. *Clin Exp Metastasis*. 2012;29(4):359–369.
24. **Cheong TC, Shin JY, Chun KH.** Silencing of galectin-3 changes the gene expression and augments the sensitivity of gastric cancer cells to chemotherapeutic agents. *Cancer Sci*. 2010;101(1):94–102.
25. **Folch J, Lees M, Sloane Stanley GH.** A simple method for the isolation and purification of total lipides from animal tissues. *J Biol Chem*. 1957;226(1):497–509.
26. **Lumeng CN, Maillard I, Saltiel AR.** T-ing up inflammation in fat. *Nat Med*. 2009;15(8):846–847.
27. **Rosen ED, Spiegelman BM.** Molecular regulation of adipogenesis. *Annu Rev Cell Dev Biol*. 2000;16:145–171.
28. **Henderson NC, Mackinnon AC, Farnworth SL, et al.** Galectin-3 regulates myofibroblast activation and hepatic fibrosis. *Proc Natl Acad Sci USA*. 2006;103(13):5060–5065.
29. **Jiang JX, Chen X, Hsu DK, et al.** Galectin-3 modulates phagocytosis-induced stellate cell activation and liver fibrosis in vivo. *Am J Physiol Gastrointest Liver Physiol*. 2012;302(4):G439–G446.
30. **Iacobini C, Menini S, Ricci C, et al.** Galectin-3 ablation protects mice from diet-induced NASH: a major scavenging role for galectin-3 in liver. *J Hepatol*. 2011;54(5):975–983.
31. **Traber PG, Zomer E.** Therapy of experimental NASH and fibrosis with galectin inhibitors. *PloS One*. 2013;8(12):e83481.
32. **Nomoto K, Tsuneyama K, Abdel et al.** Disrupted galectin-3 causes non-alcoholic fatty liver disease in male mice. *J Pathol*. 2006;210(4):469–477.
33. **Zimmermann R, Strauss JG, Haemmerle G, et al.** Fat mobilization in adipose tissue is promoted by adipose triglyceride lipase. *Science (New York, NY)*. 2004;306(5700):1383–1386.
34. **Haemmerle G, Lass A, Zimmermann R, et al.** Defective lipolysis and altered energy metabolism in mice lacking adipose triglyceride lipase. *Science (New York, NY)*. 2006;312(5774):734–737.